A C G publications

Org. Commun. 16:1 (2023) 24-34

organic communications

Synthesis of some piperazine/piperidine amides of chromone-2-carboxylic acid as potential soluble epoxide hydrolase (sEH) inhibitors

Tugce Gur Maz [1*] and Huseyin Burak Caliskan [2]

[1]*Gazi University, Faculty of Pharmacy, Department of Pharmaceutical Chemistry, 06530, Ankara, Türkiye*

[2] *TOBB ETU Economy and Technology University, Faculty of Engineering, Department of Biomedical Engineering, 06560, Ankara, Türkiye*

(Received February 10, 2022; Revised March 02, 2023; Accepted March 04, 2023)

Abstract: Inhibition of soluble epoxide hydrolase (sEH) is implicated as a new therapeutic approach against inflammatory disorders in the context of metabolic and cardiovascular diseases. In the course of our ongoing research on sEH inhibitors, we synthesized novel piperidine/piperazine amide derivatives of the chromone-2-carboxylic acid, and evaluated their inhibitory properties against human sEH. The chemical structures of the target compounds (**2-5, 7-9**) were elucidated by means of ^{1}H-NMR, ^{13}C-NMR and HRMS spectra. Initial screening of final compounds against sEH at a final concentration of 10 μM led to the identification of compound **7**, which inhibited sEH activity in a concentration-dependent manner with an IC_{50} = 1.75 μM. Therefore, this chromone-2-amide derivative **7** decorated with benzyl piperidine on the amide side can be regarded as a novel lead structure, which pave the way of developing new analogues with improved inhibitory activities against sEH.

Keywords: Fluorometric; inhibition; piperazine; piperidine; soluble epoxide hydrolase.

1. Introduction

Soluble epoxide hydrolase (sEH, EC 3.3.2.10) is an enzyme that is associated with the biosynthesis of several lipid mediators originated from the arachidonic acid (AA) metabolism [1]. sEH is a part of the cytochrome (CYP)P450 branch of the AA pathway, which particularly catalyzes the conversion of epoxyeicosatrienoic acids (EETs) that are produced by oxidation of AA with CYP2J and CYP2C to the corresponding dihydroxy metabolites, namely dihydroxyeicosatrienoic acids (DHETs) (Figure 1) [2, 3]. EETs and DHETs have opposing biological actions in which the EETs show anti-inflammatory and vasodilatory activities, while DHETs are proinflammatory and cause vasoconstriction. Literature reports demonstrate that EETs are involved in complex biological processes to suppress inflammation, balance vascular tone, lower blood pressure, decrease the formation of reactive oxygen species (ROS) and endoplasmic reticulum (ER) stress, thereby producing beneficial pharmacological actions. There are large

* Corresponding author: E-mail: ztugcegur@gmail.com

The article was published by ACG Publications
http://www.acgpubs.org/journal/organic-communications © January-March 2023 EISSN:1307-6175
DOI: http://doi.org/10.25135/acg.oc.145.2302.2705
Available online: March 10, 2023

number of data indicating that the reduced levels of EETs as a consequence of the increased activity of sEH have been associated with various pathological responses such as inflammation, hypertension, and neurodegeneration. Therefore, inhibiting sEH to elevate biologically active endogenous EET levels with the aim to extend their beneficial actions has become a new therapeutic modality for treatment of arthritic pain, cardiovascular diseases and various disorders characterized with inflammation as well as mitochondrial disfunction [4, 5].

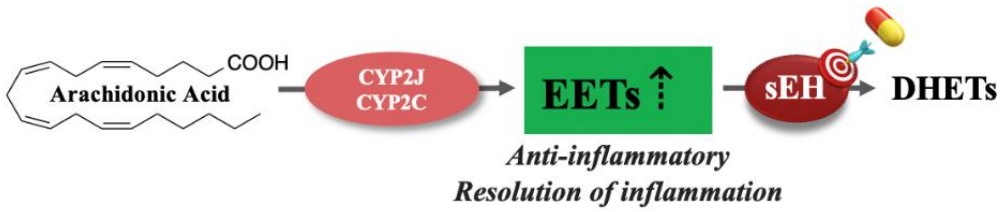

Figure 1. CYP450-mediated AA pathway highlighting sEH as potential therapeutic target

sEH has both C-terminal hydrolase and N-terminal phosphatase domains in which the hydrolysis of pharmacologically beneficial EETs to rather harmful DHETs are executed in the hydrolase domain (Figure 1) [6, 7]. The biological function of the N-terminal phosphatase domain is still not fully understood, [8, 9] however the inhibitors of sEH hydrolase domain against inflammatory and cardiovascular diseases are well studied, as exemplified with several compounds that reached to the human clinical development phase (Compounds I-IV in Figure 2) [10-12]. Moreover, a number of X-ray co-crystal structures with sEH inhibitors and also with chemical fragments disclosed that urea and amide pharmacophores in inhibitor structures are critical features to establish direct interactions in the hydrolase catalytic center [13, 14]. In particular, urea or amide groups establish H-bonding interactions to the active site catalytic residues Tyr381, Tyr465 and Asp333, thus behaving as primary pharmacophores for optimal binding interactions at the sEH active site. In addition, mainly hydrophobic/aromatic fragments around urea/amide groups are housed in the two binding areas called long and short branches. These hydrophobic and space-filling interactions at both sides altogether with the polar interactions at the catalytic center seem to stabilize the inhibitor ligands at the active site of sEH [14].

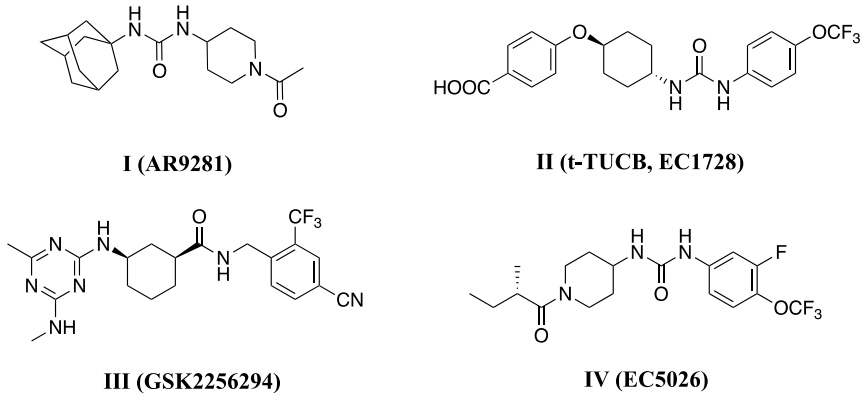

Figure 2. Examples of benchmark sEH inhibitors I–IV

With the aim to develop novel anti-inflammatory compounds, our research group recently identified quinazolinone, benzoxazolone and piperazine derivatives flanking the urea or amide pharmacophores as potent sEH inhibitors [15-17]. In the light of the structure-activity relationships obtained in these studies, we performed diversification of the heteroaryl fragment within these inhibitors and synthesized chromone-2-carboxamides as potential sEH inhibitors, which led to the identification of a prototype compound (**7**) with an IC_{50} = 1.75 μM. We therefore propose that this new chemotype is prone

to further development of an expanded set of analogs with enhanced sEH inhibition as potential anti-inflammatory agents.

2. Experimental

2.1. Chemistry

All chemicals and reagents were purchased from commercial suppliers Sigma Aldrich and BLDPharm. The newly synthesized compounds were purified by Grace Reveleris Prep system on flash chromatography mode, eluting with dichloromethane (DCM) and ethyl acetate (EtOAc) solvent system. NMR spectra were recorded on a Varian Mercury 400 MHz and Bruker 500 MHz spectrometer. Stuart SMP50 melting point apparatus was used for the determination of melting point of the compounds. High resolution mass spectroscopy (HRMS) spectra was carried on by UPLC-MS system interconnecting with time of flight (TOF) in electrospray ionization (ESI) in (+) mode. The purity of the final compounds were >97%. The chemical structures of the compounds were elucidated using ^{1}H-NMR and ^{13}C-NMR spectra which were recorded in DMSO-d_6.

2.1.1. Synthetic Procedure of the Proposed Compounds

*General Procedure for the Synthesis of **2-5**:* To a solution of commercially available **1** (1.05 mmol, 1.1 eq) in DCM, EDC.HCl (N-(3-Dimethylaminopropyl)-N′-ethylcarbodiimide hydrochloride) (1.1 eq) and DMAP (4-(Dimethylamino)pyridine) (0.2 eq) was added, and the resulting mixture was stirred at rt under N_2 atmosphere for 10 minutes. Then, appropriate piperazine derivatives (1 eq) was added to the mixture and the mixture was left to stir overnight at rt. After completion of the reaction, the mixture was partitioned between DCM and 5% $NaHCO_3$ solution. The combined organic layer was dried, filtered and evaporated under vacuo to give the crude, which was purified by flash chromatography, eluting with 100% DCM → 70% DCM in EtOAc.

*2-[4-(2-Chlorophenyl)piperazine-1-carbonyl]-4H-chromen-4-one **(2)***: Yield: 107 mg, 27.6%. White solid, Mp: 155.8-157.9 °C.^{1}H-NMR (400 MHz, DMSO-d_6): δ 3.04 (4H, bs, N-CH_2), 3.70 (2H, s, N-CH_2), 3.78 (2H, s, N-CH_2), 6.59 (1H, s, chromone H_3), 7.04-7.08 (1H, m, Ar-H), 7.17 (1H, dd, J = 7.6, 1.2 Hz, Ar-H), 7.28-7.32 (1H, m, Ar-H), 7.41 (1H, dd, J = 8.0, 1.2 Hz, Ar-H), 7.52 (1H, t, J = 7.6 Hz, Ar-H), 7.70 (1H, d, J = 8.0 Hz, Ar-H), 7.82-7.86 (1H, m, Ar-H), 8.05 (1H, dd, J = 7.6, 1.2 Hz, Ar-H); ^{13}C-NMR (100 MHz, DMSO-d_6): δ 41.9 (N-CH_2), 46.8 (N-CH_2), 50.4 (N-CH_2), 51.0 (N-CH_2), 110.7 (chromone C_3), 118.6 (chromone C_8), 121.3 (Ar-C), 123.7 (Ar-C), 124.4 (Ar-C), 124.8 (Ar-C), 125.9 (Ar-C), 127.7 (Ar-C), 128.1 (Ar-C), 130.2 (Ar-C), 134.7 (Ar-C), 148.3 (Ar-C), 155.4 (chromone -C), 157.8 (chromone -C), 160.2 (C=O) , 176.5 (C=O). HRMS (*m/z*) $[M+H]^+$ calculated for $C_{20}H_{18}ClN_2O_3$: 369.1006; found: 369.1005.

*2-[4-(2-Fluorophenyl)piperazine-1-carbonyl]-4H-chromen-4-one **(3)**:* Yield: 110 mg, 29.7%. White solid, Mp: 128.3-129.7 °C. ^{1}H-NMR (400 MHz, DMSO-d_6): δ 3.07 (4H, bs, N-CH_2), 3.70-3.77 (4H, m, N-CH_2), 6.58 (1H, s, chromone H_3), 6.97-7.15 (4H, m, fluorophenyl -H), 7.52 (1H, t, J = 7.6 Hz, chromone H_6), 7.69 (1H, d, J = 8.4 Hz, chromone H_8), 7.83 (1H, t, J = 7.6 Hz, chromone H_7), 8.05 (1H, dd, J = 7.6, 1.2 Hz, chromone H_5); ^{13}C-NMR (100 MHz, DMSO-d_6): δ 41.7 (N-CH_2), 46.5 N-CH_2), 49.7 N-CH_2), 50.3 (N-CH_2), 110.7 (chromone C_3), 115.9 (fluorophenyl, d, $^{2}J_{C\text{-}F}$ = 19.9 Hz), 118.6 (chromone C_8), 119.6 (fluorophenyl, d, $^{4}J_{C\text{-}F}$ = 2.5 Hz), 122.9 (fluorophenyl, d, $^{3}J_{C\text{-}F}$ = 7.7 Hz), 123.7 (chromone -C), 124.7 (fluorophenyl, d, $^{3}J_{C\text{-}F}$ = 3.8 Hz), 124.8 (chromone -C), 125.9 (chromone -C), 134.7 (chromone -C), 139.2 (fluorophenyl, d, $^{2}J_{C\text{-}F}$ = 8.9 Hz), 154.9 (fluorophenyl, d, $^{1}J_{C\text{-}F}$ = 242.3 Hz), 155.4 (chromone -C), 157.7 (chromone -C), 160.1 (C=O), 176.5 (C=O). HRMS (*m/z*) $[M+H]^+$ calculated for $C_{20}H_{18}FN_2O_3$: 353.1301; found: 353.1285.

*2-{4-[(2-Chlorophenyl)methyl]piperazine-1-carbonyl}-4H-chromen-4-one **(4)**:* Yield: 133 mg, 33%. Obtained as HCl salt, white solid, Mp: 224.2-226.4 °C. ^{1}H-NMR (400 MHz, DMSO-d_6): δ 3.3-3.45 (8H,

m, N-CH_2), 4.46 (2H, s, Ph-CH_2), 6.63 (1H, s, chromone H_3), 7.42-7.56 (4H, m, Ar-H), 7.66 (1H, dd, *J* = 8.8 Hz, chromone H_8), 7.82-7.86 (1H, m, Ar-H), 7.98 (1H, d, *J* = 6.0 Hz, Ar-H), 8.04 (1H, d, *J* = 8.0 Hz, chromone H_5); ^{13}C-NMR (100 MHz, DMSO-d_6): δ 43.2 (N-CH_2), 49.9 (N-CH_2), 50.6 (N-CH_2), 55.5 (Ph-CH_2), 111.2 (chromone C_3) , 118.6 (chromone C_8), 123.7 (Ar-C), 124.8 (Ar-C), 125.9 (Ar-C), 127.5 (Ar-C), 129.7 (Ar-C), 131.4 (Ar-C), 133.9 (Ar-C), 134.6 (Ar-C), 134.7 (Ar-C), 155.4 (chromone -C), 156.7 (chromone -C), 160.3 (C=O), 176.5 (C=O). HRMS (*m/z*) $[M+H]^+$ calculated for $C_{21}H_{20}ClN_2O_3$: 383.1162; found: 383.1180.

*2-{4-[(3-Chlorophenyl)methyl]piperazine-1-carbonyl}-4H-chromen-4-one (**5**):* Yield: 98 mg, 24.3%. Obtained as HCl salt, white solid, Mp: 240-242.2 °C. ^{1}H-NMR (400 MHz, DMSO-d_6): δ 3.1-3.3 (8H, m, N-CH_2), 4.34 (2H, s, Ph-CH_2), 6.61 (1H, s, chromone H_3), 7.44-7.54 (3H, m, Ar-H), 7.58 (1H, d, *J* = 6.4 Hz, Ar-H), 7.66 (1H, d, *J* = 8.8 Hz, Ar-H), 7.77 (1H, s, Ar-H), 7.82-7.86 (1H, m, Ar-H), 8.03 (1H, d, *J* = 8.0 Hz, chromone H_5); ^{13}C-NMR (100 MHz, DMSO-d_6): δ 43.0 (N-CH_2), 49.8 (N-CH_2), 50.3 (N-CH_2), 57.8 (Ph-CH_2), 111.2 (chromone C_3), 118.6 (chromone C_8), 123.7 (Ar-C), 124.8 (Ar-C), 125.9 (Ar-C), 129.4 (Ar-C), 130.1 (Ar-C), 130.5 (Ar-C), 131.2 (Ar-C), 133.2 (Ar-C), 134.7 (Ar-C), 155.4 (chromone -C), 156.7 (chromone -C), 160.3 (C=O), 176.5 (C=O). HRMS (*m/z*) $[M+H]^+$ calculated for $C_{21}H_{20}ClN_2O_3$: 383.1162; found: 383.1162.

*4-Oxo-N-(piperidin-4-yl)-4H-chromene-2-carboxamide **(6)**: step i)* To a solution of **1** (1.05 mmol, 1.1 eq) in DCM, 4-amino-*N*-Boc piperidine (1 eq), EDC.HCl (1.1 eq) and DMAP (0.2 eq) was added and the resulting mixture was stirred at rt under N_2 atmosphere overnight. After completion of the reaction, the mixture was partitioned between DCM and 5% $NaHCO_3$ solution. The combined organic layer was dried, filtered and evaporated under vacuo to give tert-butyl 4-(4-oxo-4*H*-chromene-2-amido)piperidine-1-carboxylate which was triturated in EtOAc, then filtered and used for the next step without further purification. *step ii)* To a solution of tert-butyl 4-(4-oxo-4*H*-chromene-2-amido)piperidine-1-carboxylate (1 eq) in DCM, trifluoroacetic acid (TFA) (1 eq) was added and stirred at rt for 2 hours. Then, the reaction mixture was partitioned between DCM and 5% $NaHCO_3$ solution. The combined organic layer was dried, filtered and evaporated to give the crude which was used for the next step. Yield: overall 2 steps, 42.8%. Obtained as oil. HRMS (*m/z*) $[M+H]^+$ calculated for $C_{15}H_{17}N_2O_3$: 273.1239; found: 273.1228.

*4-Oxo-N-(1-{[2-(trifluoromethyl)phenyl]methyl}piperidin-4-yl)-4H-chromene-2-carboxamide (**7**):* To a solution of **6** (100 mg, 0.36 mmol, 1 eq) in ACN, 2-(trifluoromethylbenzyl bromide (1.2 eq) and K_2CO_3 (2.5 eq) was added, and the resulting mixture was heated at 50 °C for 4 hours. After completion of the reaction, the mixture was evaporated in vacuo. Then, it was partitioned between DCM and 5% $NaHCO_3$ solution. The combined organic layer was dried, filtered and evaporated under vacuo to give the crude which was purified by flash chromatography, eluting with 100% DCM → 70% DCM in EtOAc. Yield: 51 mg, 32.2%. White solid, Mp: 185.1-186.4 °C. ^{1}H-NMR (500 MHz, DMSO-d_6): δ 1.69-1.74 (2H, m, piperidine H_3), 1.81 (2H, d, *J* = 11.6 Hz, piperidine H_3), 2.13 (2H, t, *J* = 11.6 Hz, piperidine H_2), 2.82 (2H, d, *J* = 11.6 Hz, piperidine H_3), 3.64 (2H, s, Ph-CH_2), 3.78-3.88 (1H, m, piperidine H_4), 6.83 (1H, s, chromone H_3), 7.47 (1H, t, *J* = 7.55 Hz, Ar-H), 7.53 (1H, t, *J* = 7.5 Hz, Ar-H), 7.65-7.71 (2H, m, Ar-H),7.77 (2H, d, *J* = 8.25 Hz, Ar-H), 7.90 (1H, td, *J* = 7.75, 1.6 Hz, chromone H_7), 8.05 (1H, dd, *J* = 7.95, 1.45 Hz, chromone H_5), 8.91 (1H, d, *J* = 7.95 Hz, -NH); ^{13}C-NMR (125 MHz, DMSO-d_6): δ 31.6 (piperidine C_3), 47.6 (piperidine C_4), 52.7 (piperidine C_2), 58.2 (Ph-CH_2), 111.0 (chromone C_3), 119.4 (chromone C_8), 124.1 (chromone -C), 124.9 (q, $^1J_{C\text{-}F}$ = 272.4 Hz, Ar-C), 125.4, 126.2 (q, $^3J_{C\text{-}F}$ = 5.6 Hz, Ar-C), 126.5, 127.7 (q, $^2J_{C\text{-}F}$ = 29.6 Hz, Ar-C), 127.8 (Ar-C), 130.8 (Ar-C), 132.9 (Ar-C), 135.4 (Ar-C), 138.3 (Ar-C), 155.6 (chromone -C), 156.2 (chromone -C), 158.8 (C=O), 177.8 (C=O). HRMS (*m/z*) $[M+H]^+$ calculated for $C_{23}H_{22}FN_2O_3$: 431.1583; found: 431.1575.

*N-{1-[(2-chlorophenyl)methyl]piperidin-4-yl}-4-oxo-4H-chromene-2-carboxamide (**8**):* It was prepared from 2-chlorobenzyl bromide (1.2 eq) under the conditions that was used in preparation of compound **7.** White solid, Mp: 167.2-168.7 °C. Yield: 21.2 mg, 14.5%. ^{1}H-NMR (500 MHz, DMSO-d_6): δ 1.67-1.73 (2H, m, piperidine H_3), 1.81 (2H, d, *J* = 11.6 Hz, piperidine H_3), 2.16 (2H, t, *J* = 11.6 Hz, piperidine H_2), 2.87 (2H, d, *J* = 11.6 Hz, piperidine H_2), 3.59 (2H, s, Ph-CH_2), 3.82-3.84 (1H, m, piperidine H_4), 6.83 (1H, s, chromone H_3), 7.28-7.31 (1H, td, *J* = 7.7, 1.65 Hz, Ar-H), 7.35 (1H, td, *J* = 7.4, 1.2 Hz, Ar-H),

7.44 (1H, dd, *J* = 7.8, 1.2 Hz, Ar-H), 7.50 (1H, dd, *J* = 7.5, 1.55 Hz, Ar-H), 7.54 (1H, td, *J* = 8.0, 0.9 Hz, Ar-H), 7.79 (1H, d, *J* = 8.0 Hz, Ar-H), 7.88-7.91 (1H, m, Ar-H), 8.05 (1H, dd, *J* = 7.95, 1.65 Hz, chromone H_5), 8.90 (1H, d, *J* = 7.95 Hz, -NH); ^{13}C-NMR (100 MHz, DMSO-d_6): δ 31.0 (piperidine C_3), 47.1 (piperidine C_4), 52.1 (piperidine C_2), 58.5 (Ph-CH_2), 110.4 (chromone C_3), 118.8 (chromone C_8), 123.6 (Ar-C), 124.8 (Ar-C), 125.9 (Ar-C), 126.9 (Ar-C), 128.5 (Ar-C), 129.2 (Ar-C), 130.6 (Ar-C), 133.2 (Ar-C), 134.8 (Ar-C), 135.9 (Ar-C), 155.1 (chromone -C), 155.7 (chromone -C), 158.3 (C=O), 177.2 (C=O). HRMS (*m/z*) $[M+H]^+$ calculated for $C_{22}H_{22}ClN_2O_3$: 397.1319; found: 397.1338.

*N-[1-(2-methoxypyridine-3-carbonyl)piperidin-4-yl]-4-oxo-4H-chromene-2-carboxamide (**9**):* It was prepared from compound **6** (1 eq) and 2-methoxynicotinic acid (1.1 eq) under the same manner that was used in preparation of compound **2.** Yield: 32 mg, 17.8%. White solid, Mp: 248-250.4 °C.^{1}H-NMR (500 MHz, DMSO-d_6): δ 1.47-1.99 (4H, m, piperidine H_3), 2.89-3.21 (2H, m, piperidine -H), 3.28-3.37 (1H, m, piperidine -H), 3.93 (3H, s, -OCH_3), 4.10 (1H, bs, piperidine -H), 4.53 (1H, bs, piperidine -H), 6.85 (1H, s, chromone H_3), 7.09 (1H, s, pyridine H_5), 7.54 (1H, t, *J* = 7.85 Hz, chromone H_6), 7.66 (1H, dd, *J* = 7.25, 1.7 Hz, chromone H_6), 7.78 (1H, s, pyridine H_4), 7.90 (1H, td, *J* = 7.55, 1.55 Hz, chromone H_7), 8.05 (1H, dd, *J* = 7.95, 1.4 Hz, chromone H_5), 8.25 (1H, s, pyridine H_6); 8.90 (1H, d, *J* = 7.95 Hz, -NH); ^{13}C-NMR (125 MHz, DMSO-d_6): δ 31.2 (piperidine C_3), 31.9 (piperidine C_3), 45.7 (piperidine C_2), 47.4 (piperidine C_4), 53.9 (OCH_3), 111.1 (chromone C_3), 117.7 (chromone C_8), 119.4 (pyridine -C_3), 120.3 (pyridine -C_5), 124.1 (chromone -C), 125.4 (chromone -C), 126.5 (chromone -C), 135.5 (chromone -C), 137.5 (pyridine -C_4), 147.9 (pyridine -C_6), 155.6 (chromone -C), 156.1 (chromone -C), 158.9 (C=O), 159.2 (C=O), 165.0 (pyridine -C_2), 177.8 (C=O). HRMS (*m/z*) $[M+H]^+$ calculated for $C_{22}H_{22}N_3O_5$: 408.1559; found: 408.1561.

2.2. Biological Activity

The sEH assay kit was purchased from Cayman Chemical (Item no: 10005196). The described assay protocol was followed to evaluate sEH inhibition of the target compounds. Briefly, 185 µL of assay buffer (125 mM Tris-HCl, pH 9.0, 1 mM EDTA) was loaded into each well in which 5 µL of inhibitor was then added. Later, 5 µL of diluted enzyme and 5 µL of substrate PHOME was added to initiate the reaction, subsequently. The plate was incubated at rt for 15 minutes. The hydrolysis of PHOME by sEH was given fluorescent response which was recorded at Ex= 355 nm and Em= 465 nm by Biotek Synergy H1 hybrid microplate reader, respectively.

2.3. Molecular Modeling

Molecular docking simulations were run in Schrödinger Maestro (Version 12.8.117, Release 2021-2). The crystal structure of sEH with bound ligand was uploaded from RCSB PDB (ID 7A7G). Protein was prepared with Schrödinger's Protein Preparation Wizard. Ligand was prepared with the LigPrep. The OPLS4 force field was used. Docking was run in SP mode with a scaling factor 0.85 for van der Waals radii. Solvent molecules were retained during simulations. In order to verify binding parameters, bound ligand in the X-ray structure (referred here as co-ligand) was first tested in dockings until superposition of the co-ligand with all its interactions was observed. The same parameters were then used for subsequent simulations. All other parameters were unchanged and default settings were used unless stated otherwise.

3. Results and Discussion

3.1. Chemistry

The synthetic route for the compounds were depicted in Scheme 1 and 2. The chemical structure of the target compounds were elucidated with ^{1}H-NMR, ^{13}C-NMR an HRMS analysis. The physical data and HRMS analysis are reported in Table 1. The reactions were carried out in the same manner as reported literatures [18].

Table 1. Melting point and HRMS analysis results of the compounds **(2-5, 7-9)**

#	Mp (°C)	Molecular Formula	HRMS *m/z* [M+H] $^+$	
			Calculated	Found
2	155.8-157.9	$C_{20}H_{17}ClN_2O_3$	369.1006	369.1005
3	128.3-129.7	$C_{20}H_{17}FN_2O_3$	3531301	353.1285
4	224.2-226.4	$C_{21}H_{19}ClN_2O_3$	383.1162	383.1180
5	240-242.2	$C_{21}H_{19}ClN_2O_3$	383.1162	383.1162
7	185.1-186.4	$C_{23}H_{21}FN_2O_3$	431.1583	431.1575
8	167.2-168.7	$C_{22}H_{21}ClN_2O_3$	397.1319	397.1338
9	248-250.4	$C_{22}H_{21}N_3O_5$	408.1559	408.1561

For the synthesis of compound **2-5,** to the solution of the commercially available chromone-2-carboxylic acid (**1**) in DCM was added appropriate phenyl/benzyl piperazine derivatives in the presence of EDC.HCl and DMAP to produce desired compounds (Scheme 1).

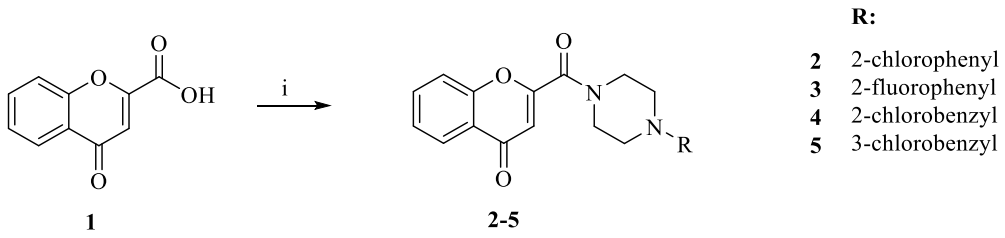

1 **2-5**

Scheme 1. Reagent and conditions: *i)* EDC.HCl, DMAP, appropriate piperazine derivatives, DCM, rt, overnight

Compound **6** bearing piperidine moiety was obtained by the amide coupling of the starting compound **1** with 4-amino-N-Boc piperidine, which was subsequently deprotected in the presence of TFA. Compounds **7** and **8** were then obtained by alkylation of the common intermediate **6** with 2-trifluoromethylbenzyl bromide and 2-chlorobenzyl bromide, respectively, in the presence of K_2CO_3 in acetonitrile (ACN). Compound **9** was obtained by the amide coupling of intermediate **6** with 2-methoxynicotinic acid (Scheme 2).

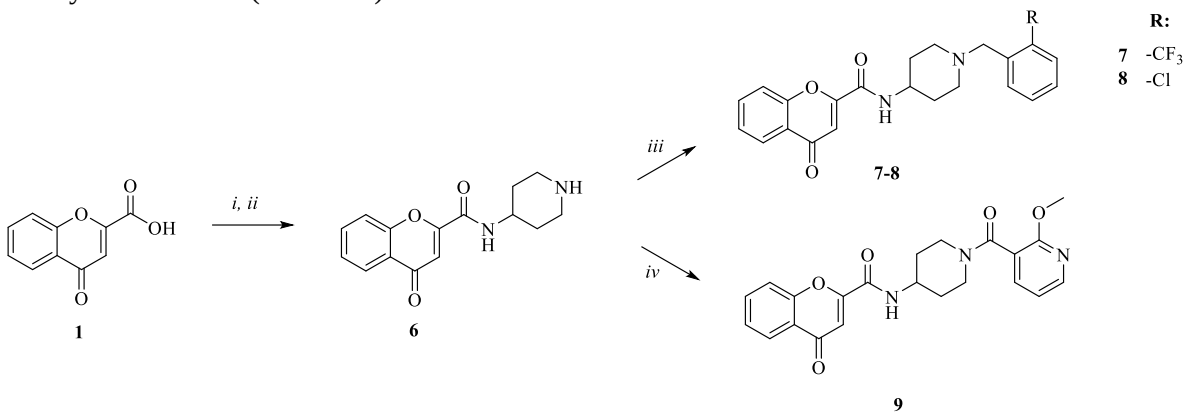

1 **6** **7-8** **9**

Scheme 2. Reagent and conditions: *i)* EDC.HCl, DMAP, 4-amino-*N*-Boc piperidine, DCM, rt, overnight; *ii)* TFA, DCM, rt, 2h; *iii)* appropriate benzyl bromides, K_2CO_3, ACN, 50 °C, 5h; *iv)* 2-methoxynicotinic acid, EDC.HCl, DMAP, DCM, rt, overnight

3.2. Biological Activity

The inhibitory activities of the final compounds against human sEH were evaluated using the Soluble epoxide hydrolase inhibitor screening assay kit (Cayman, U.S.A.). Initial screening of the final compounds was performed at 10 μM in the final assay conditions as (Figure 3). Compounds **2-5**, tertiary amide derivatives obtained with phenyl and benzylpiperazines, were found to inhibit sEH in the range of 25-40%. However, compounds **7-9**, secondary amide derivatives obtained with 4-amino-1-benzylpiperidines, more potently inhibited the sEH activity with more than 50% inhibition at 10 μM screening concentration. Compound **7** with 1-(2-trifluoromethylbenzyl)piperidine fragment at the amide part demonstrated the most potent inhibition (~78%), which could be explained by the presence of an H-bond donor NH function in the secondary amide group and also with the appropriately substituted benzyl function at the right-end side of the molecules.

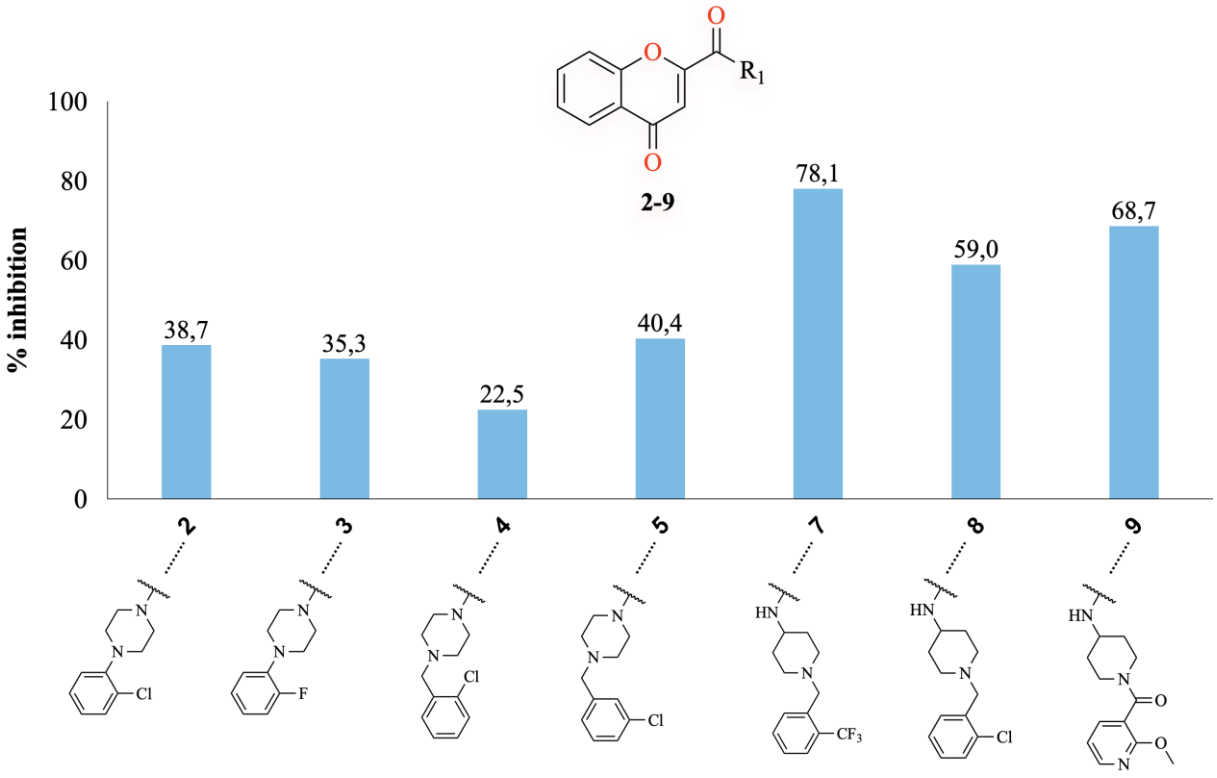

Figure 3. % inhibition of the target compounds @10 μM

Since compound **7** was the most potent analogue in the initial screening at 10 μM, its IC_{50} value was calculated to show that it concentration-dependently inhibited sEH with an IC_{50}= 1.75 μM (Figure 4). These findings indicate that this scaffold can be further developed for improved sEH inhibitors as future studies.

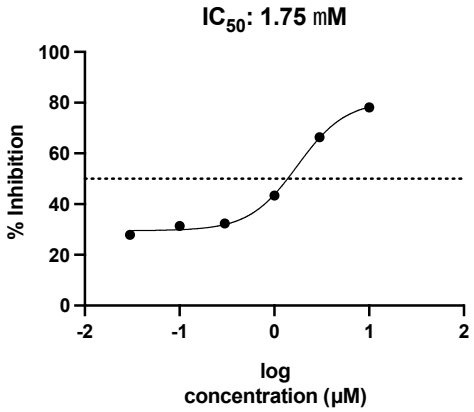

Figure 4. IC_{50} determination of the compound **7**

3.3. Molecular Modeling

In light of the elucidated active site properties of sEH in published X-ray co-crystal structures, we performed molecular docking studies to explore the favorable ligand interactions of the most potent analogue **7** at the sEH active site (PDB ID: 7A7G). As shown in Figure 5A and B, compound **7** interacts with the catalytic center through its amide group in an analogy to the reported amide-type sEH inhibitors, which anchor the compound **7** in the narrow passage of the L-shaped active site. According to this, the carbonyl oxygen establishes H-bonding interaction to Tyr383 and Tyr466, and the amide NH group forms H-bond with the Asp335. In addition, the trifluoromethylbenzyl group is accommodated in a hydrophobic pocket in the long branch as often targeted by known inhibitors to establish good binding affinity. Moreover, the piperidine ring neatly align with the Trp336 to establish cation-π interactions with its protonated nitrogen atom and further stabilizes the binding of **7** in this region. Moreover, the chromone ring of **7** binds at the bottleneck of the active site toward the short branch, establishing π-π interactions with the His524, and the binding is further stabilized by additional π-π interactions with the Trp525. Altogether, the observed interactions may explain the inhibition potential of the compound **7** to lock into binding site of the enzyme, which prevents the access of the endogenous lipid substate of the enzyme to the active site.

A

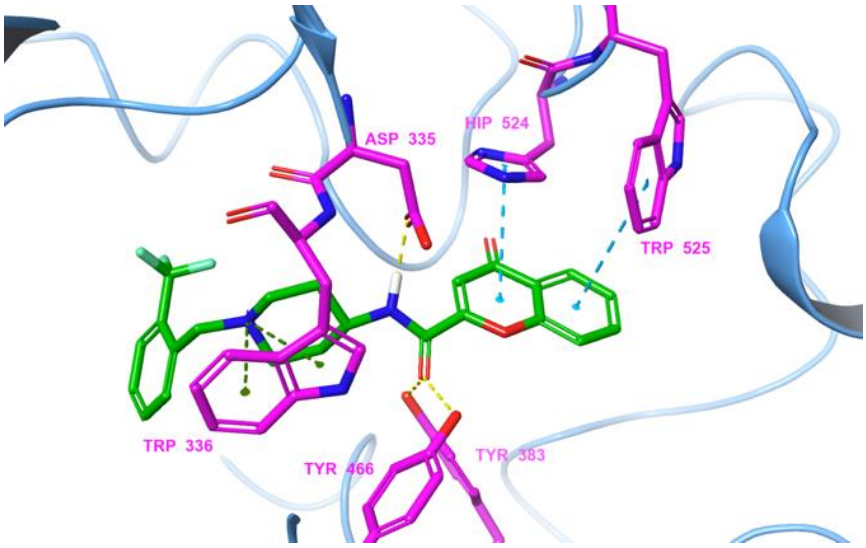

B

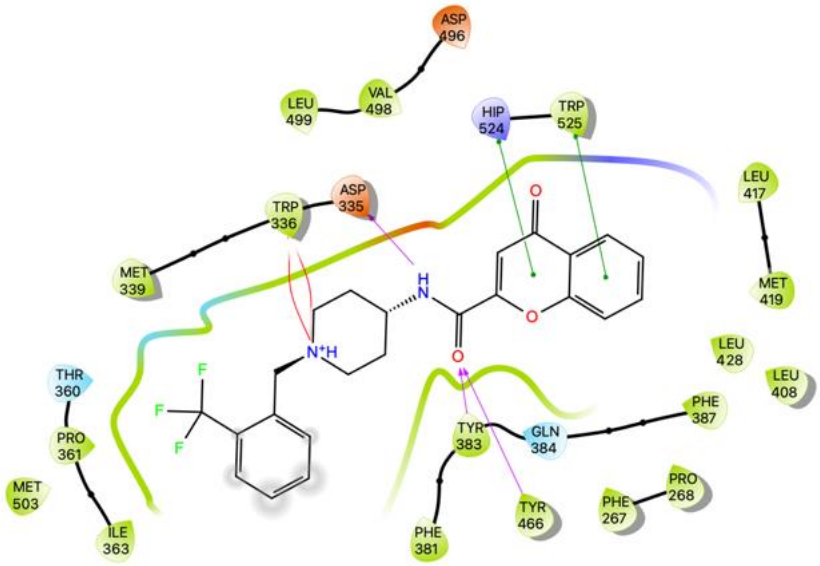

Figure 5. A) The molecular docking of **7** (green) at sEH active site (Blue ribbon structure shows the enzyme where key residues interacting with the ligand are shown in purple. Bonds are color-coded as follows: Aromatic H-bonds: light blue, H-bonds: yellow, and pi-cation bonds: dark green. PDB ID 7A7G). B) The 2D ligand interaction diagram of **7** with residues in the sEH active site (Bonds are color-coded as follows: Aromatic H-bonds: green, H-bonds: purple, and pi-cation bonds: red.)

4. Conclusion

The reported structural features of various of amide-type sEH inhibitors demonstrate that these compounds hold on to the binding site with their amide group as a main pharmacophore that establishes stable H-bonding interactions with three central residues, i.e., Asp335, Tyr383 and Tyr466, at the bottleneck of the active site. In addition, hydrophobic or aromatic groups flanking the amide pharmacophore to stabilize the binding interactions with additional aromatic or space-filling interactions at the active site. Based on this information, we hereby postulated a new inhibitor scaffold by incorporating chromone ring to the one side of the amide core along with the aryl-piperazine or piperidines at the other side. As a result, the chromone-carboxamide template generated developable potent inhibitory activity against sEH by forming expected H-bonding and aromatic interactions in the central cavity and short branch, respectively, imitating the similar interaction of pattern of the reported co-crystal ligands. Moreover, the 2-substituted benzyl group at the other side of the amide pharmacophore was also significant for steering the inhibitory activity and can be further investigated to optimize and enhance the observed hydrophobic interactions.

Consequently, the chromone ring can be considered as a secondary pharmacophore to the central amide function, paving the way for further exploitation to validate its potential use in the design of enhanced sEH inhibitors. Moreover, compound **7** can be regarded as a new lead compound for the evolution of new analogs with increased activity along with better drug-like properties.

Acknowledgements

The authors thank the Lokman Hekim University for providing the ELISA reader for biological activity studies.

Supporting Information

Supporting information accompanies this paper on http://www.acgpubs.org/journal/organic-communications

ORCID

Tugce Gur Maz: 0000-0001-8916-2492
Hüseyin Burak Çalışkan: 0000-0002-2549-1390

References

[1] El-Sherbeni, A. A.; El-Kadi, A. O. The role of epoxide hydrolases in health and disease. *Arch. Toxicol.* **2014,** *88*(*11*), 2013-32.
[2] Kroetz, D. L.; Zeldin, D. C. Cytochrome P450 pathways of arachidonic acid metabolism. *Curr. Opin. Lipidol.* **2002,** *13*(*3*), 273-83.
[3] Spector, A. A.; Kim, H. Y. Cytochrome P450 epoxygenase pathway of polyunsaturated fatty acid metabolism. *Biochim. Biophys. Acta* **2015,** *1851*(*4*), 356-65.
[4] McReynolds, C.; Morisseau, C.; Wagner, K.; Hammock, B. Epoxy Fatty Acids Are Promising Targets for Treatment of Pain, Cardiovascular Disease and Other Indications Characterized by Mitochondrial Dysfunction, Endoplasmic Stress and Inflammation. *Adv. Exp. Med. Biol.* **2020,** *1274*, 71-99.
[5] McReynolds, C. B.; Hwang, S. H.; Yang, J.; Wan, D.; Wagner, K.; Morisseau, C.; Li, D.; Schmidt, W. K.; Hammock, B. D. Pharmaceutical Effects of Inhibiting the Soluble Epoxide Hydrolase in Canine Osteoarthritis. *Front. Pharmacol.* **2019,** *10*, 533.
[6] Cronin, A.; Mowbray, S.; Durk, H.; Homburg, S.; Fleming, I.; Fisslthaler, B.; Oesch, F.; Arand, M. The N-terminal domain of mammalian soluble epoxide hydrolase is a phosphatase. *Proc. Natl. Acad. Sci. U. S. A.* **2003,** *100*(*4*), 1552-7.
[7] Morisseau, C.; Hammock, B. D. Epoxide hydrolases: mechanisms, inhibitor designs, and biological roles. *Annu. Rev. Pharmacol. Toxicol.* **2005,** *45*, 311-33.
[8] Kramer, J.; Proschak, E. Phosphatase activity of soluble epoxide hydrolase. *Prostaglandins Other Lipid Mediators* **2017,** *133*, 88-92.
[9] Kramer, J. S.; Woltersdorf, S.; Duflot, T.; Hiesinger, K.; Lillich, F. F.; Knoll, F.; Wittmann, S. K.; Klingler, F. M.; Brunst, S.; Chaikuad, A., et al. Discovery of the first in vivo active inhibitors of the soluble epoxide hydrolase phosphatase domain. *J. Med. Chem.* **2019,** *62*(*18*), 8443-8460.
[10] Chiamvimonvat, N.; Ho, C. M.; Tsai, H. J.; Hammock, B. D. The soluble epoxide hydrolase as a pharmaceutical target for hypertension. *J. Cardiovasc. Pharmacol.* **2007,** *50*(*3*), 225-37.
[11] Duflot, T.; Roche, C.; Lamoureux, F.; Guerrot, D.; Bellien, J. Design and discovery of soluble epoxide hydrolase inhibitors for the treatment of cardiovascular diseases. *Expert Opin. Drug Discov* **2014,** *9*(*3*), 229-43.
[12] Fang, X.; Singh, P.; Smith, R. G. Soluble Epoxide hydrolase as a therapeutic target for cardiovascular diseases. *Drugs Future* **2009,** *34*(*7*), 579-585.
[13] Amano, Y.; Yamaguchi, T.; Tanabe, E. Structural insights into binding of inhibitors to soluble epoxide hydrolase gained by fragment screening and X-ray crystallography. *Bioorg. Med. Chem.* **2014,** *22*(*8*), 2427-34.
[14] Bzowka, M.; Mitusinska, K.; Hopko, K.; Gora, A. Computational insights into the known inhibitors of human soluble epoxide hydrolase. *Drug Discov. Today* **2021,** *26*(*8*), 1914-1921.
[15] Capan, I.; Jordan, P. M.; Olgac, A.; Caliskan, B.; Kretzer, C.; Werz, O.; Banoglu, E. Discovery and optimization of piperazine urea derivatives as soluble epoxide hydrolase (sEH) inhibitors. *ChemMedChem* **2022,** *17*(*12*), e202200137.
[16] Gur Maz, T.; Koc, B.; Jordan, P. M.; Ibis, K.; Caliskan, B.; Werz, O.; Banoglu, E. Benzoxazolone-5-Urea Derivatives as Human Soluble Epoxide Hydrolase (sEH) Inhibitors. *ACS Omega* **2023,** *8*(*2*), 2445-2454.
[17] Turanli, S.; Ergul, A. G.; Jordan, P. M.; Olgac, A.; Caliskan, B.; Werz, O.; Banoglu, E. Quinazoline-4(3H)-one-7-carboxamide derivatives as human soluble epoxide hydrolase inhibitors with developable 5-lipoxygenase activating protein inhibition. *ACS Omega* **2022,** *7(41)*, 36354-36365.

[18] Sunkur, M.; Aydin, S.; Aral, T.; Dag, B.; Erenler, R. Preparation of new mono- and bis-amide derivatives of L-isoleucine via amidation of carboxyl and amino groups. *Org. Commun.* **2021,** *14*(*3*), 294-299.